

Novel Miniplate Designs to Enhance Biomechanical Stability in Mandibular Symphyseal Fracture Fixation

Majid Zeinalnezhad^b, Amin Dadashi^c, Akbar Allahverdizadeh^b, Behnam Dadashzadeh^{a*}

^a Department of Design and Engineering, Faculty of Science and Technology, Bournemouth University, UK

^b Department of Mechatronics Engineering, Faculty of Mechanical Engineering, University of Tabriz, Iran

^c Department of Mechanical Engineering, Tarbiat Modares University, Iran

* bdadashzadeh@bournemouth.ac.uk

Abstract

In this article, the performance of different geometries of specially designed fixation miniplates for mandibular symphyseal fracture is evaluated by investigating the effect of geometrical parameters on the biomechanical stability of the fracture. Experimental cone beam computed tomography (CBCT) images were used to generate and simulate the mandible model. Two novel miniplate geometries, including rectangular and elliptical designs, are presented to achieve better biomechanical performance than conventional design. Performance of each geometric design is evaluated in six different dimensional parameters to determine the appropriate parameters for the new miniplate designs. Three-dimensional stress analysis is performed to investigate the mechanical behavior of the novel miniplates, and the results are compared with the classic miniplate. The results reveal that the relative displacement in the symphysis bone of the fractured mandible area fixed by the new rectangular and elliptical designs is reduced 9.55% and 15.4%, respectively. In addition, the novel designs for miniplates reduce the number of screws by two in comparison to classic miniplates. The biomechanical advantages observed, such as reduced relative displacement and a decreased number of screws (implying less surgical trauma to the bone), suggest that the novel miniplate designs hold the potential to contribute to more favorable clinical outcomes, possibly influencing aspects such as patient recovery time. Findings of this research provide a foundation for future experimental and clinical investigations of potential clinical benefits.

Keywords: Fixation miniplate, Mandible, Symphysis, Fracture, 3D stress analysis

1. Introduction

A traumatic fracture of the mandible can lead to dysphagia, inability to retain saliva, speech disorders, and aesthetic disfigurement ¹. On average, 42% of facial and jaw fractures occur in the mandible, as it is the skull's largest and only movable bone ². Fractures of the mandible in the symphysis or parasymphysis are relatively common and account for almost 20% of mandibular fractures ³. 75% of fractures occur in men aged 20 to 30 years ⁴ and are often due to physical altercations.

For precise open surgical procedures, a thorough examination is essential to diagnose dental trauma, trigeminal nerve function, lacerations, airway compromise, and associated injuries. Imaging is usually performed with a multi-slice computed tomography (CT) scan. A panoramic radiograph is also commonly used, but some symphyseal fractures may be missed if not carefully examined. The key to successfully treating these fractures lies in understanding the principles of accurate restoration of occlusion and stable internal fixation. Studies have shown that the correct placement of miniplate along Champi's optimal osteosynthesis lines leads to good patient results ³. Open surgery and internal fixation (OSIF) is used to stabilize the fractured segments ⁵. Miniplates are required to perform the operation. Miniplates are usually thin pieces of titanium or stainless steel that are attached directly to the bone segments with metal screws ^{6,7}. The thickness of the miniplates is in the order of millimeters ⁵.

Mandibular fractures are usually associated with facial trauma, and almost half of the patients require surgery ^{4,8}. Open surgical procedures aim to restore the pre-injury structure and regain normal function. In order to achieve proper function, the alignment of the maxillary and mandibular teeth to each other, known as the occlusal surface (occlusion), must be taken into account ⁹. 18% of patients undergoing mandibular fracture treatment suffer from a condition known as occlusal misalignment, which is due to displacement of the fracture site during healing and is more common in patients with mandibular or midface fractures ^{10,11}. This condition may result from improper placement or loosening of the plates/screws during treatment ^{5,11}. Another study investigated the titanium miniplate's efficacy and postoperative complications in mandibular fractures (parasymphyseal, symphyseal, mandibular body, and angle). Patients were examined regularly up to 2 months after surgery. The results indicated that using titanium miniplates was effective in treating mandibular fractures ¹².

Finite element analysis (FEA) can effectively simplify the mechanical behavior of structures under complex loading by using numerical methods to analyze and simulate structural behavior ¹³. FEA can play an essential role in investigating the mechanics of mandibular fractures. Finite

element analysis can be used to study the miniplate's size, thickness, geometry, or specific structure¹⁴ and to determine the most appropriate shape for treating a specific type of fracture in the mandible¹⁵.

Due to the physiological complexity of the masticatory system, muscle forces cannot be measured empirically and, therefore, determined by mathematical models. For this purpose, physiological information such as muscle length, origin, direction, and attachment point are required. This data was obtained by examining several bodies¹⁶ or by MRI scans^{17,18}. To investigate the mechanical behavior of miniplates in the mandible, the type and magnitude of forces acting on the system under investigation are essential. Bending and torsional forces are exerted by several muscles in the mandibular bone during chewing. The type and magnitude of forces required to investigate the mechanical behavior of the miniplate in the mandible bone were utilized based on the results of previous research¹⁹.

Based on the previous results of studies, influential factors in the use of miniplates for treating mandibular fractures include the geometry, dimensions, and the number of screws required to fix the miniplate to the bone. This article introduces two innovative designs with rectangular and elliptical geometries for the first time. The study's innovation lies in the proposal of new geometries designed to lower stress levels in the mandible bone, reduce the required number of screws to fix the miniplate to the bone, minimize damage to the mandible bone, and enhance overall performance compared to current miniplates. A 3D mandible model was constructed from a CT scan of a 30-year-old male patient to evaluate the performance of the proposed miniplate designs. The Mimix software was utilized to generate the mandible geometry based on the bone tissue's Hounsfield Unit (HU) values. A benchmark classic miniplate with eight screws was considered for comparison. The novel designs incorporated six screws and were analyzed in six different geometries with varying dimensions to determine the proper configuration. The mandible bone and the miniplate stress distribution were assessed using finite element analysis (FEA). The effects of geometric parameters and screw placement on stress distribution were evaluated. The overall dimensions of the proposed miniplate geometries were maintained to ensure compatibility with existing surgical procedures.

2. Materials and methods

The mandible, also known as the lower jaw, is a complex bone that plays a crucial role in mastication, speech, and facial support. Understanding the biomechanics of the mandible is essential for developing effective treatment strategies for various craniofacial disorders. Finite

element analysis is a computational method that can be used to simulate the stresses and strains within the mandible under various loading conditions. To perform FEA, a detailed geometric model of the mandible is required.

2.1. Geometry of mandible

In this study, a geometric model of the mandible was constructed from CBCT images of a 30-year-old male patient. The CBCT scans were acquired using a NewTom VGi system with a slice thickness of 0.3 mm, a spacing of 0.3%, and a 512×512 pixels resolution. The selected sample had 419 sections. The images were saved in 419 different files in DICOM file format. The individual DICOM files were imported into the Mimics software for segmentation. A bone mask was created based on Hounsfield unit (HU) thresholding. Three-dimensional (3D) models of the mandible were generated in the axial, coronal, and sagittal planes to ensure the accuracy of the model. The teeth were ignored to reduce computational complexity. Finally, a surface mesh file in STL format was exported (Fig. 1). The surface mentioned is imported to Geomagic design software, and a volume file with STP format is created. The completed geometric model of the mandible was imported into Abaqus FEA software.



Fig. 1. Surface model of the mandible generated using the patient's CBCT images in Mimics software.

2.2. Novel miniplates design

In order to investigate the mechanical behavior of a fractured mandible, a thorough crack in the mid-symphyseal region was considered in the geometric model of the mandible. Three miniplate models were examined in this study:

- A classic (conventional) miniplate, as shown in Fig. 2,
- A novel rectangular miniplate design, as exhibited in Fig. 3,
- A novel elliptical miniplate design, as illustrated in Fig. 4,

The classic miniplate was positioned in the mid-symphysis region of the mandible. The classic and new miniplate thickness was maintained at 1 (mm), a standard size for these types of implants. This thickness provides sufficient strength while minimizing bone damage during insertion. The diameter of the screw holes in all miniplates was set to 2 millimeters, ensuring compatibility with standard surgical screws.

Their overall dimensions were kept consistent to facilitate a fair comparison between the classic and new miniplate designs. The classic and new miniplates had a length of 28 (mm) and a height of 18 (mm). This standardization ensures that the performance evaluation is based solely on geometric variations, not overall size differences. Maintaining consistent overall dimensions across the classic and new miniplates allows for a controlled assessment of the effects of geometric variations. By isolating the influence of geometry, which specific geometric features contribute to improved stress distribution and performance can be accurately determined. Fig. 2 illustrates the specific dimensions of the classic miniplate (Classic).

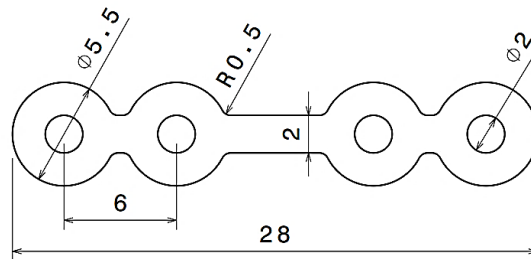


Fig. 2. Classic miniplate dimensions used in previous studies ²⁰.

New designs Rectangular (Fig. 3) and elliptical (Fig. 5) miniplates were evaluated using six geometric parameters, each labeled R1 to R6 (Table 1) and E1 to E6 (Table 2), respectively. In the Rectangular miniplate, the effect of two length parameters named a and b was investigated, and in the Elliptical miniplate, two angle parameters named α and β were examined.

For R1, R2, and R3 miniplates, the width of the lateral recess is varied as $a = 4,6,8$ (mm), while for R4, R5, and R6, this dimension is fixed at 4 (mm), and the width of the central gap is varied as $b = 1.4,0.7,0$ (mm). For E1, E2, and E3 miniplates, the angle of the screw hole is

varied as $\alpha = 20^\circ, 40^\circ, 60^\circ$, which $\beta = 40^\circ$ is fixed, and for E4, E5, and E6, angle α is fixed at 40 degrees, and the angle of the middle arm is varied as $\beta = 20^\circ, 35^\circ, 50^\circ$. Notably, the diameter of all holes in all miniplates under consideration is assumed to be a constant value of 2 millimeters.

The rectangular miniplate design was based on the main geometric parameters, a , b , c , and d , as exhibited in Fig. 3. These main geometric parameters include six parameters, which are summarized in Table 1 and marked with a , b , c , and d .

Table 1 Geometric parameters of the proposed rectangular design.

Case	a (mm)	b (mm)	c (mm)	d (mm)
R1	4	2.1	2.1	9
R2	6	2.1	2.1	9
R3	8	2.1	2.1	9
R4	4	1.4	2.8	8.3
R5	4	0.7	3.5	7.6
R6	4	0	4.2	6.9

In the geometric design of rectangular miniplates, the values of the fixed geometric parameters in all six configurations are determined in Fig. 3. Rectangular miniplates were designed in six configurations, as shown in Fig. 4. It should be noted that the positions of the screw holes in the rectangular miniplates are symmetry concerning the vertical symmetrical axis.

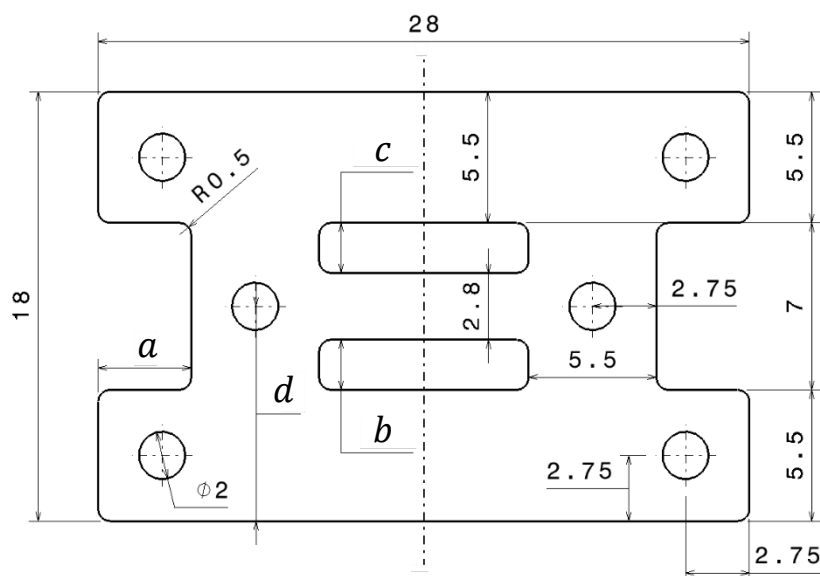


Fig. 3. Geometric parameters of the proposed rectangular miniplate design.

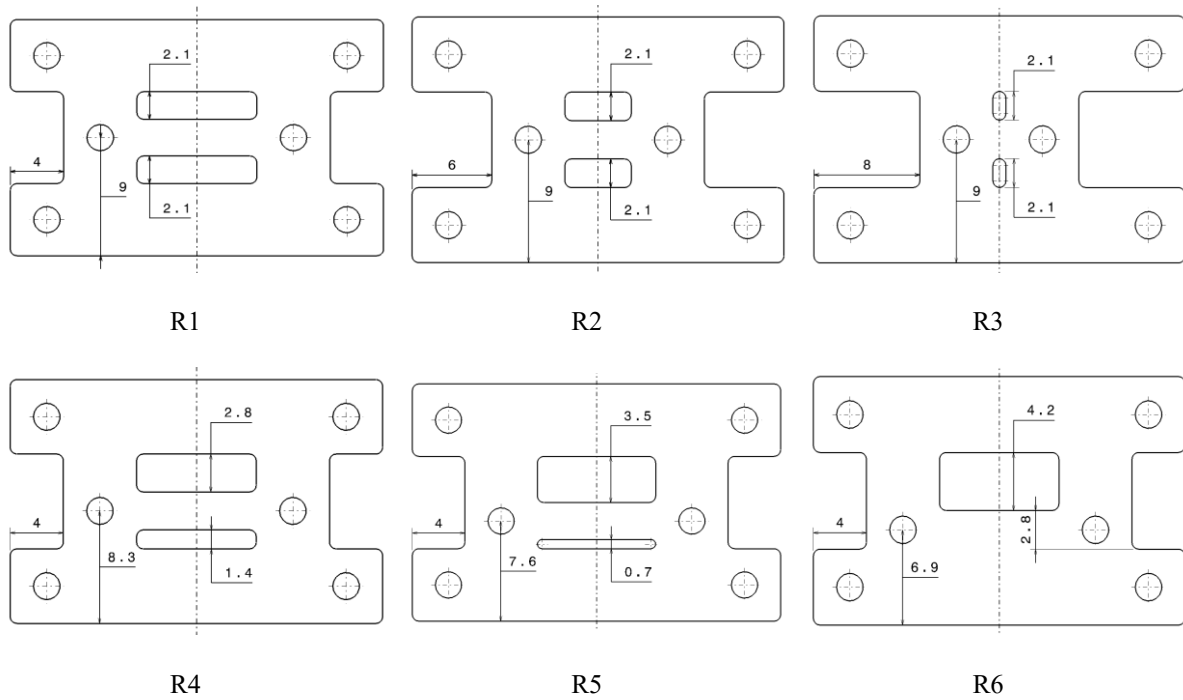


Fig. 4. The geometric parameters of six rectangular miniplate configurations (dimensions in mm).

The elliptical miniplate design was based on the main geometric parameters, angles α and β , as exhibited in Fig. 5. These main geometric parameters include six parameters, which are summarized in Table 2 and marked with α and β . It is important to note that the positions of the screw holes in the elliptical miniplate are symmetry with respect to the horizontal and vertical symmetrical axes of the elliptical shape.

In the geometric design of elliptical miniplates, the values of the fixed geometric parameters in all six configurations are determined in Fig. 5. Elliptical miniplates were designed in six configurations, as shown in Fig. 6.

Table 2 Geometric parameters of the proposed elliptical design.

Case	α (deg)	β (deg)
E1	20°	40°
E2	40°	40°
E3	60°	40°
E4	40°	20°
E5	40°	35°
E6	40°	50°

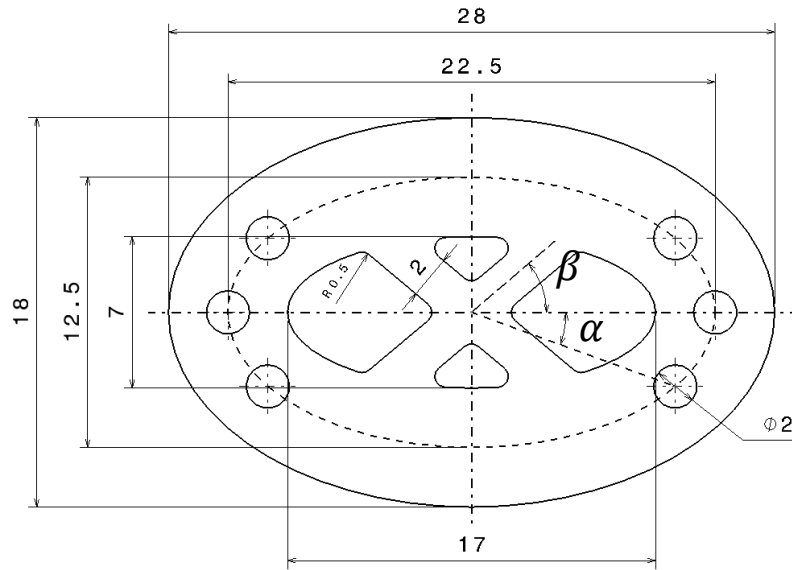


Fig. 5. Geometric parameters of the proposed elliptical miniplate design (dimensions in mm).

All proposed miniplate designs underwent thorough analysis and evaluation. The classic design (Fig. 7a) utilized two conventional miniplates, each 1 (mm) thick, secured with eight 9-(mm) screws. Rectangular (Fig. 7b) employed the rectangular miniplate, also 1 (mm) thick, fastened with six 9-millimeter screws. Finally, elliptical (Fig. 7c) featured the elliptical miniplate, 1 (mm) thick, secured with six 9-millimeter screws. In the stress analysis, these miniplates possess curvatures that mimic the anatomy of the mandibular symphysis.

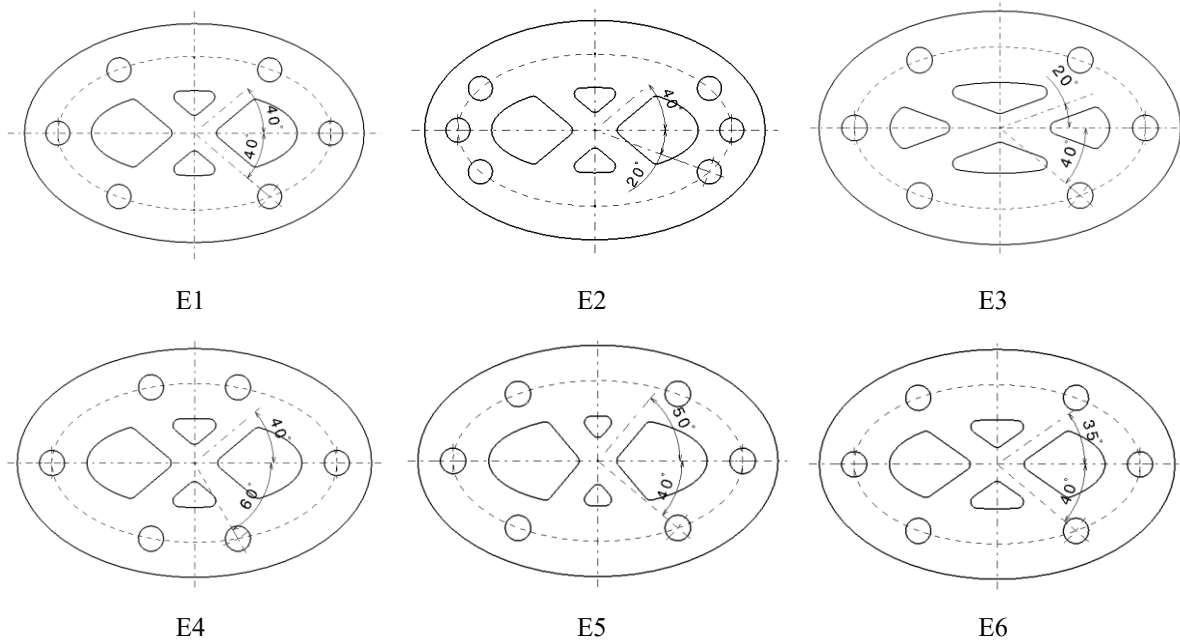


Fig. 6. The geometric parameters of six elliptical miniplate configurations.

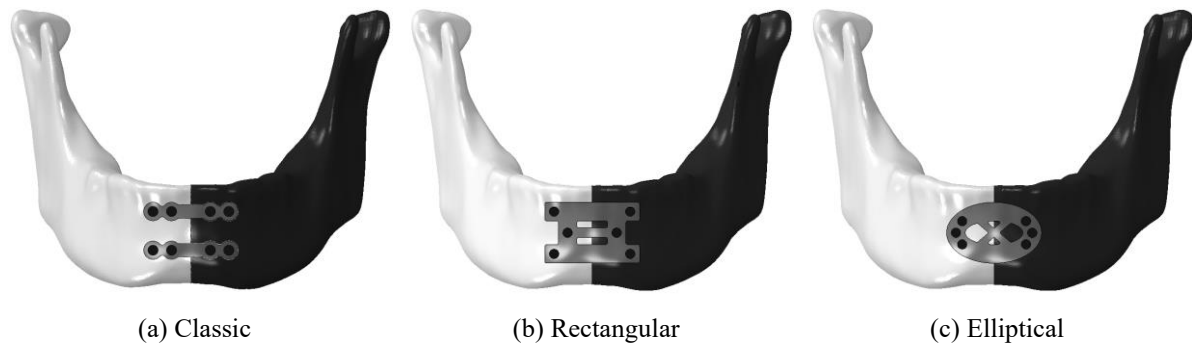


Fig. 7. Assembled of miniplates and screws in the fractured mandible (a) Classic miniplate used in previous studies, (b) Rectangular miniplate with the new design, (c) Elliptical miniplate with the new design.

As illustrated in Fig. 7, the mandible bone is consistently represented with its two segments in differing shades of grey. This consistent representation across all analyzed scenarios highlights the assumption that the mandible has sustained a fracture in the symphysis region.

2.3. Mandible's muscles forces

Crafting an accurate biomechanical model of the mandible necessitates a thorough understanding of the forces exerted upon it by the masticatory muscles. These forces are instrumental in driving mandibular movement and function. Therefore, a comprehensive analysis of the forces generated by all relevant muscles is paramount. According to existing literature^{21,22}, nine bilateral muscles contribute to the forces acting on the mandible. These muscles, meticulously listed in Table 3, comprise the Superficial Masseter, Deep Masseter, Medial Pterygoid, Anterior Temporalis, Middle Temporalis, Posterior Temporal, Inferior Lateral Pterygoid, Superior lateral pterygoid, and Anterior Digastric.

Table 3 The name and location of the muscles of the mandible.

No.	Muscle Name	Muscle Location
1	Superficial Masseter	Right, left
2	Deep Masseter	Right, Left
3	Medial Pterygoid	Right, left
4	Anterior Temporalis	Right, left
5	Middle Temporalis	Right, left
6	Posterior Temporal	Right, left
7	Inferior Lateral Pterygoid	Right, left
8	Superior lateral pterygoid	Right, left
9	Anterior Digastric	Right, Left

The magnitudes and directions of the considered muscle forces were based on the work of Nelson et al.²¹. Nelson's study is considered a benchmark for muscle forces and has been used as a standard in many previous FEA studies attempting to simulate the mandible's mechanical behavior²³⁻²⁶. The data from this reference is for a healthy adult with a healthy jaw. It has been

estimated that the muscle force values for a patient with a mandibular fracture are 60% of those of a healthy adult ²⁷. The force data was modified accordingly in this study. The muscle attachment points to the mandible were determined based on the reference ²⁸. The muscle forces were applied in the simulation according to their geometric positions, as shown in Fig. 8.

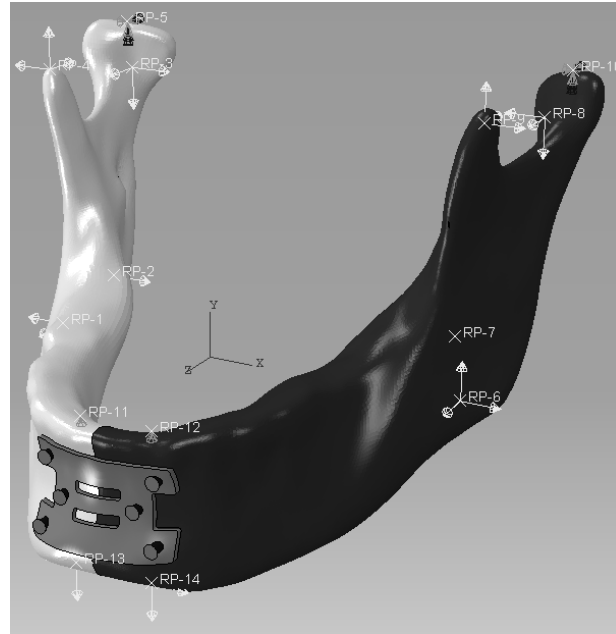


Fig. 8. Loads and boundary conditions on the model.

The direction cosines that describe the direction of muscle forces are provided in Table 4. The magnitudes and directions of the muscle forces are determined by Eq. (1).

$$M_{ir} = [X_{Mi} \cdot K]EMG_{Mi} \quad (1)$$

where X_{Mi} represents the cross-sectional area of the muscle attachment in (cm^2), and K is a general scaling constant for skeletal muscle expressed in (N/cm^2). The product $[X_{Mi} \cdot K]$ is referred to as the weighting factor (N) and indicates the maximum possible muscle force for a muscle. The term EMG_{Mi} serves as a scaling factor for each biting task, scaling down the muscle force in proportion to the maximum possible muscle force exerted by a particular muscle group. The M_{ir} obtained from Eq. (1) represents the magnitude of the muscle force for a specific muscle. These forces were then distributed to the nodes attached to each muscle attachment area in the model. Symmetrical bilateral clenching is the main type of bite force analyzed in this study (Table 5) ²⁹.

Table 4 Muscle weight factors [$X_{Mi} \cdot K$] for each masticatory muscle group and direction cosines of muscle direction components ^{21,26}.

Masticatory Muscles	Weighting Factor (N)	Right Side Direction Cosines			Left Side Direction Cosines		
		Cos-x	Cos-y	Cos-z	Cos-x	Cos-y	Cos-z
Superficial Masseter	190.4	-0.207	0.884	0.419	0.207	0.884	0.419
Deep Masseter	81.6	-0.546	0.758	-0.358	0.546	0.758	-0.358
Medial Pterygoid	174.8	0.486	0.791	0.372	-0.486	0.791	0.372
Anterior Temporalis	158	-0.149	0.988	0.044	0.149	0.988	0.044
Middle Temporalis	95.6	-0.221	0.837	-0.5	0.221	0.837	-0.5
Posterior Temporal	75.6	-0.208	0.474	-0.855	0.208	0.474	-0.855
Inferior Lateral Pterygoid	66.9	0.63	-0.174	0.757	-0.63	-0.174	0.174
Superior lateral pterygoid	28.7	0.761	0.074	0.645	-0.761	0.074	0.645
Anterior Digastric	40	-0.244	-0.237	-0.94	0.244	-0.237	-0.94

Table 5 Left and right muscle scale factors of bilateral clenching, EMG_{Mi} ²¹.

Masticatory Muscles	Bilateral Symmetrical Clenching	
	Right	Left
Superficial Masseter	1	1
Deep Masseter	1	1
Medial Pterygoid	0.76	0.76
Anterior Temporalis	0.98	0.98
Middle Temporalis	0.96	0.96
Posterior Temporal	0.94	0.94
Inferior Lateral Pterygoid	0.27	0.27
Superior lateral pterygoid	0.59	0.59
Anterior Digastric	0.28	0.28

2.4. Mechanical Properties of the Materials

Ever since titanium alloys were introduced for dental implants around 1981, there has been a significant increase in their usage to replace missing teeth in patients ^{30,31}. Modern titanium-based dental implants have a high success rate and are rarely associated with complications or failure ³¹. There are various titanium alloys available, with one of the newest being Ti-6Al-4V. Due to its superior strength and lower Young's modulus, Ti-6Al-4V is used in various types of implants, especially dental implants, and its use is biologically acceptable ³²⁻³⁴. Tests conducted on this type of alloy show that the tensile yield stress is in the range of 800-850 (MPa), and the ultimate tensile strength is 900-950 (MPa) ^{32,35,36}. In this investigation, the material for miniplates and screws was considered from Ti-6Al-4V titanium alloy with Young's modulus of 113 (GPa) and Poisson's ratio (ν) of 0.34 ³⁴. The mandible, which is composed of cortical bone, is assumed to have linear elastic, homogeneous, and isotropic behavior with mechanical properties of $E = 13.7$ (GPa) and $\nu = 0.3$ ³⁷. Cortical bone has an ultimate tensile strength

ranging from 92 to 188 (MPa) and an ultimate compressive strength of 133 to 295 (MPa) ²². The von Mises criterion is used to evaluate the stress state in the mandible and miniplates.

2.5. Mesh Independence Study

Before finalizing the results, a mesh independence study was conducted to ensure that the results were not significantly affected by the number of elements in the finite element model. The finite element model for the mandible with the rectangular miniplate was meshed using five different mesh densities: 27210, 33610, 104365, 165456, and 395584 elements. Quadratic tetrahedral elements were used for the bone regions, and quadratic hexahedral elements were used for the miniplate and screw geometries. Fig. 9 shows an example of the meshing for the model with 395584 elements.

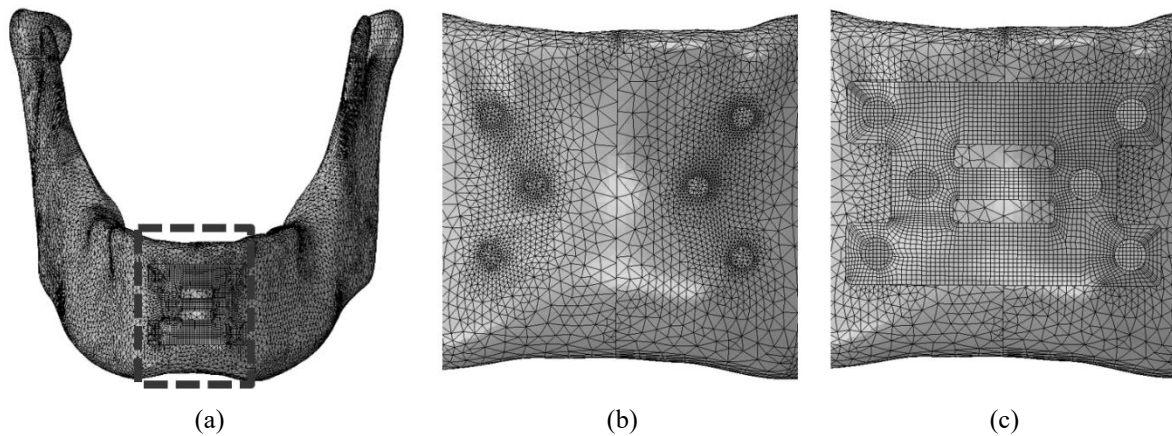


Fig. 9. (a) The meshing of the finite element model with 395584 elements, (b) The density of elements in the area around the location of the screws in the symphysis, (c) The density of elements in rectangular miniplate.

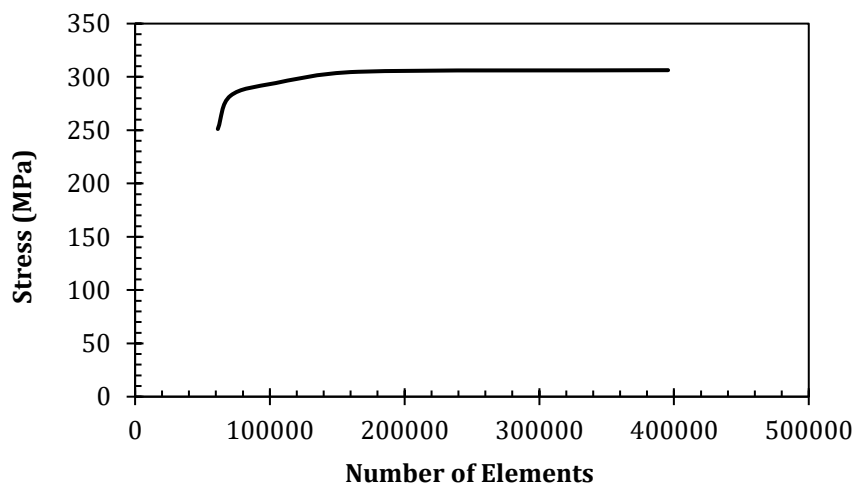


Fig. 10. Convergence analysis of von Mises stress using finite element method.

Fig. 10 shows the convergence of the maximum von Mises stress values obtained from the numerical analyses for the different mesh densities with the specified number of elements. The convergence plot indicates that the von Mises stress values become independent of the number of elements for mesh densities greater than 165,000 elements.

3. Results and Discussion

Thirteen different miniplate geometries were studied to investigate their impact on the mechanical behavior of a fractured mandible. To thoroughly investigate the stress and displacement distribution, one representative configuration from each miniplate category (classical, rectangular, and elliptical) was selected. For the remaining cases, key parameters such as maximum von Mises stress in the mandible, miniplate, and screws, along with maximum relative displacement between the fractured bone fragments, were reported for comparison.

Three-dimensional finite element (FE) analyses were conducted to investigate the stress and strain distribution in a fractured mandible fixed with different miniplate geometries. The mandible model was subjected to physiological loading conditions, including muscle forces and boundary conditions. It is important to note that the following results present stress distributions in megapascals (MPa) and displacement distributions in millimeters (mm) using contour legends for visual interpretation.

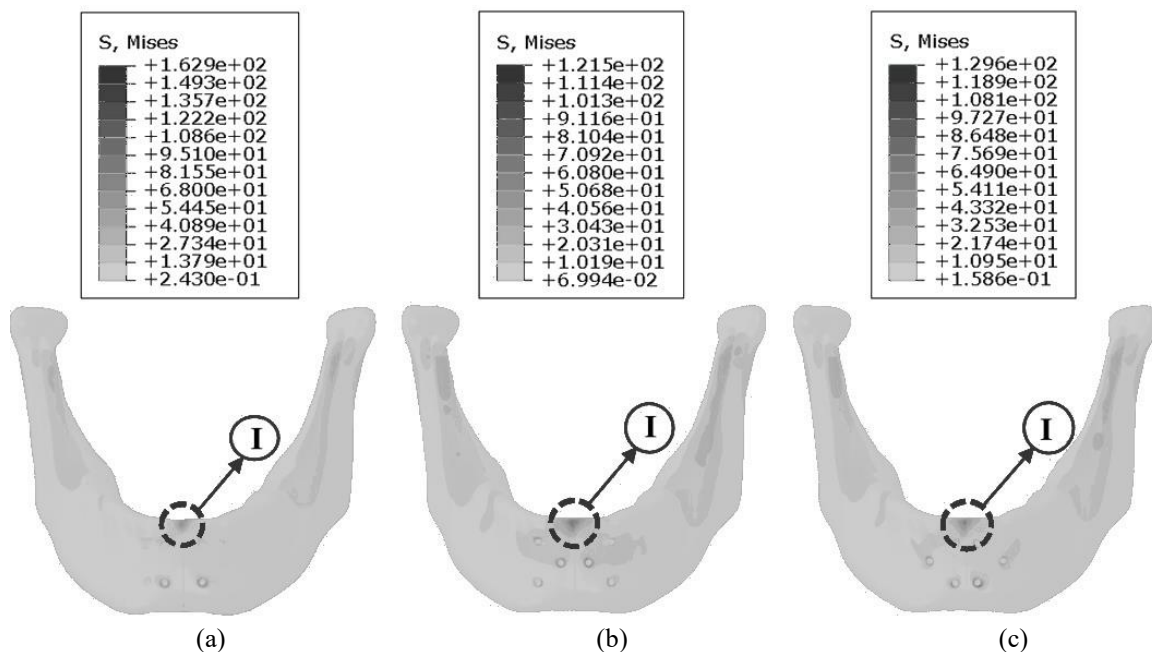


Fig. 11. Von Mises stress in MPa in the mandibular bone fixed using (a) the classic miniplate, (b) rectangular R3 miniplate, (c) elliptical E3 miniplate.

At first, classic miniplates are analyzed. Fig. 11a illustrates the von Mises stress distribution in the mandible when the miniplate classic is used. The maximum von Mises stress in the mandible is 162.9 (MPa), occurring in the superior region of the mandible, denoted by the "I" symbol in Fig. 11a. In this region, the fractured edges of the mandible are subjected to compressive forces due to the applied muscle forces and boundary conditions.

As illustrated in Fig. 12a, the region "I" exhibiting the maximum von Mises stress value also coincides with the lowest minimum principal stress location. In this region, the minimum principal stress is negative, reaching a value of -238.4 (MPa). This observation highlights the relationship between von Mises's stress and principal stress distribution. Von Mises stress is a scalar quantity representing the equivalent stress for a material subjected to a complex stress state. The minimum principal stress, on the other hand, represents the smallest of the three principal stresses at a point. In the classic miniplate configuration, the negative minimum principal stress values in the maximum von Mises stress regions suggest significant compressive stress. It is important to note that, in general, there are three principal stresses at each point in the computational domain: the first principal stress, the second principal stress, and the third principal stress. According to the default naming convention in Abaqus software, the smallest principal stress, considering its sign, is identified as the Min Principal stress.

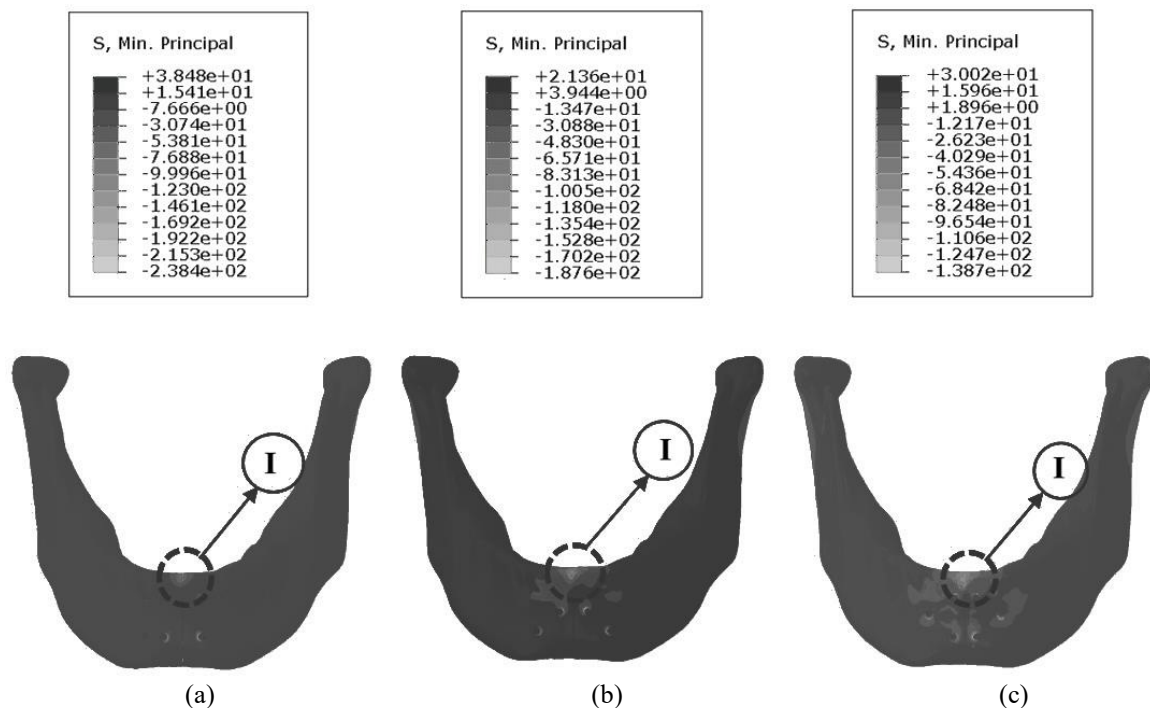


Fig. 12. Minimum principal stress in MPa in the mandibular bone fixed using (a) the classic miniplate, (b) rectangular R3 miniplate, (c) elliptical E3 miniplate.

Fig. 13a depicts the displacement field of the mandible with miniplates in the case where the mandible is stabilized using classic miniplates. The image is enlarged ten times to emphasize the displacements around the fracture. The relative displacement between the fracture surfaces is a crucial factor in evaluating miniplate efficacy in mandible fixation. Minimizing relative displacement between the fracture surfaces promotes the healing process. In this case, the maximum relative displacement between the two fractured surfaces at the posterior aspect of the mandibular symphysis region is 0.272 (mm).

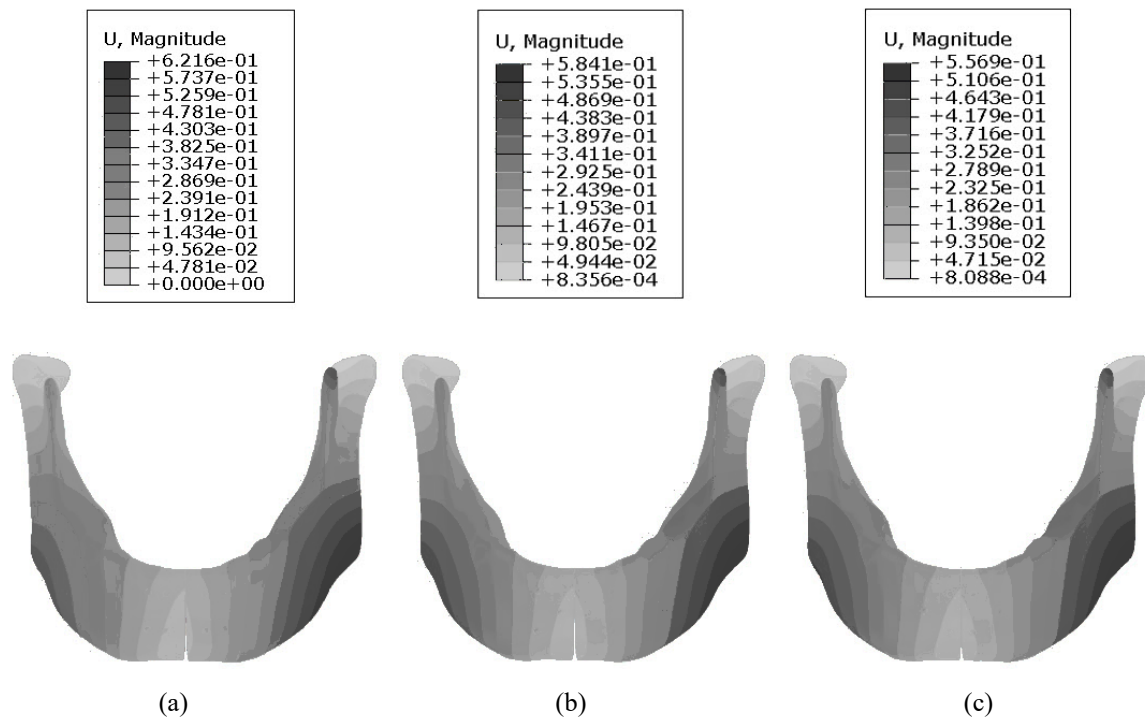


Fig. 13. Displacement distribution in the mandible with 10x magnification fixed using (a) the classic miniplate, (b) rectangular R3 miniplate, (c) elliptical E3 miniplate.

Fig. 14a illustrates the von Mises stress distribution on the miniplate's anterior and posterior surfaces. It is evident that the miniplate situated on the inferior aspect of the mandible bears a higher stress. Within this miniplate, the peak von Mises stress is observed near the holes, reaching a value of 526.9 (MPa), which falls within titanium's elastic range^{32,35,36}.

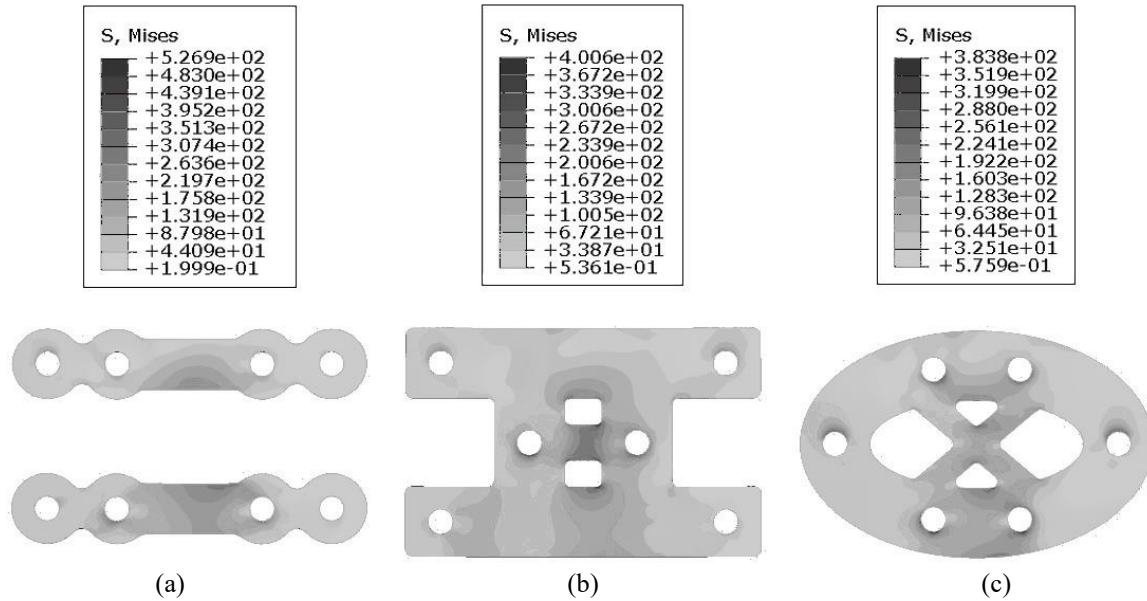


Fig. 14. Von Mises stress distribution in MPa in the back side of (a) the classic miniplate, (b) rectangular R3 miniplate, (c) elliptical E3 miniplate, used for mandible fixation.

Fig. 11b demonstrates the von Mises stress distribution in the mandible for the third design of the novel rectangular miniplates (R3). The maximum Von Mises stress of 121.5 (MPa) occurs in the superior region of the mandible, denoted by region "I" in Fig. 11b. This region experiences compression between the two fractured bone surfaces due to the applied muscle forces and boundary conditions. The stress analysis results indicate that the R3 design effectively distributes stresses within the mandible. The maximum von Mises stress of 121.5 (MPa) is smaller than the compressive strength of cortical bone, which is approximately 214 (MPa) ²². This suggests that the R3 design can withstand the applied loads without plastic deformation.

The minimum principal stress distribution in the mandible for the third design of the novel rectangular miniplates (R3) is exhibited in Fig. 12b. The minimum principal stress of -187.6 (MPa) occurs in the superior region of the mandible, denoted by Region I in Fig. 12b. The minimum principal stress of -187.6 (MPa) is smaller than the compressive strength of cortical bone, which is approximately 214 (MPa) ²².

The magnified (10x) displacement field in the mandible for the third design of the novel rectangular miniplates (R3) is shown in Fig. 13b. The maximum relative displacement between the two fractured surfaces occurs at the posterior region of the symphysis, with a value of 0.246 (mm).

The results of the displacement field analysis indicate that the R3 design effectively stabilizes the fractured mandible. The maximum relative displacement of 0.246 (mm) is within the acceptable range for bone healing, suggesting that the R3 design can provide sufficient stability for proper bone healing. The R3 design helps distribute the stresses in this area, which may reduce the risk of displacement and promote mandibular bone healing.

The von Mises stress distribution in the miniplate for the third design of the novel rectangular miniplates (R3) is shown in Fig. 14b. The maximum von Mises stress of 400.6 (MPa) occurs in the central region of the miniplate. The maximum von Mises stress of 400.6 (MPa) is below the yield stress of titanium alloy, which is approximately 825 (MPa)^{32,35,36}. This suggests that the R3 design can withstand the applied loads without plastic deformation of the miniplate. The stress concentration in the central region of the miniplate is due to the complex loading applied to the miniplate. The R3 design distributes these loads across the width of the miniplate, reducing the stress concentration compared to the classic miniplate.

The maximum von Mises stress of 253.1 (MPa) occurs in the shank of the screw, near the head of the screw (Fig. 15a). The maximum Von Mises stress of 253.1 (MPa) is smaller than the yield strength of titanium alloy, which is approximately 825 (MPa)^{32,35,36}. This suggests that the R3 design can withstand the applied loads without plastic deformation in the screws.

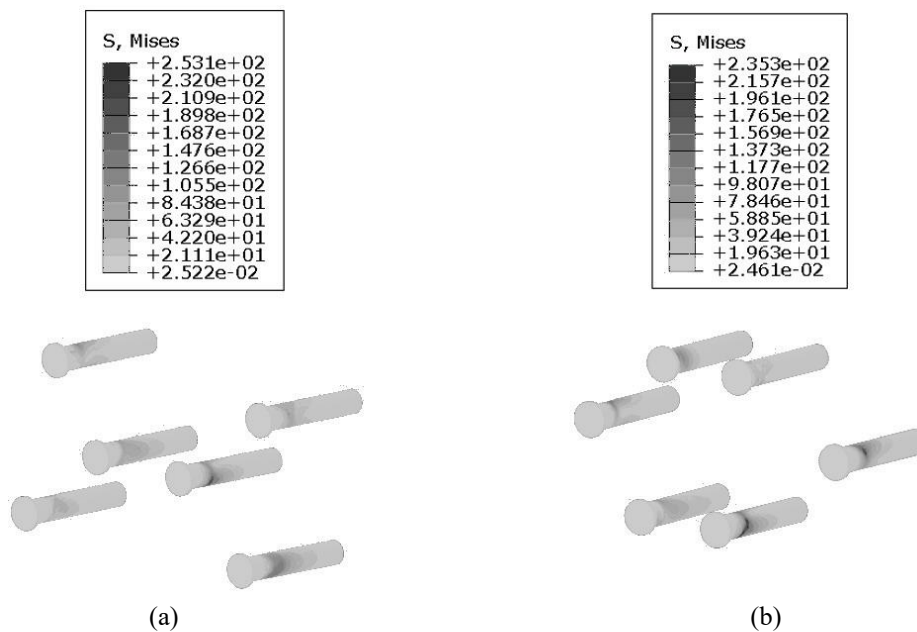


Fig. 15. Von Mises stress distribution in MPa in the screws used for fixing, (a) rectangular R3 miniplate, (b) elliptical E3 miniplate.

In the following stress analysis, the stress distribution within the mandible is investigated using the third design of the novel elliptical miniplate (E3). Fig. 11c illustrates the von Mises stress distribution, revealing a maximum stress of 129.6 (MPa) in the superior region of the mandible (region I). This area experiences compression due to the combined effects of applied muscle forces and the boundary conditions imposed on the fractured bone segments. The stress analysis results indicate that the E3 design effectively distributes stresses throughout the mandible. The maximum von Mises stress of 129.6 (MPa) remains below cortical bone's compressive strength, typically around 214 (MPa) ²². The E3 design's ability to distribute stresses in this area may contribute to a more favorable environment for bone healing.

Fig. 12c presents the minimum principal stress distribution within the mandible for the third design of the novel elliptical miniplates (E3). The analysis reveals a minimum principal stress of -138.7 (MPa) in the superior region of the mandible (region I). The stress analysis results are encouraging, indicating that the E3 design effectively distributes stresses throughout the mandible. The minimum principal stress of -138.7 (MPa) remains well smaller than cortical bone's compressive strength, typically around 214 (MPa) ²². This suggests that the E3 design can successfully withstand the applied loads without incurring structural failure.

Fig. 13c presents the magnified (10x) displacement field within the mandible for the third design of the novel elliptical miniplates (E3). The analysis reveals a maximum relative displacement of 0.230 (mm) between the two fractured surfaces, occurring in the posterior region of the symphysis. The maximum displacement observed in the posterior region of the symphysis is attributed to the complex biomechanical loading in this area. The E3 design's ability to distribute displacements in this region may contribute to a more favorable environment for bone healing.

The von Mises stress distribution in the miniplate is illustrated in Fig. 14c. The maximum von Mises stress of 383.8 (MPa) occurs in the back of the middle region of the miniplate. This suggests that the miniplate is under significant stress in this area. It is important to note that titanium alloy's yield strength, the material typically used for miniplates, is around 825 (MPa) ^{32,35,36}. This suggests that the miniplate can withstand the applied loads without plastic deformation.

The von Mises stress distribution within the screws of the third-generation elliptical miniplate design (E3) is exhibited in Fig. 15b. As observed, the maximum stress of 235.3 (MPa) is

localized in the shank region near the screw head. This value remains well smaller than the yield strength of titanium alloy, typically around 825 (MPa) ^{32,35,36}.

Table 6 summarizes the key findings from the finite element analysis of all investigated scenarios, including the maximum von Mises stress in the mandible bone, miniplate, and screws, along with the maximum relative displacement between the two fractured mandibular segments. The von Mises stress for the rectangular miniplate exhibits the most considerable reduction in case R4, while the elliptical miniplate achieves the lowest stress for the E3 design.

Table 6 The highest von Mises stress in the mandible bone, miniplate, and screws and its percentage changes compared to the classic miniplate (Classic).

Miniplates	The highest von Mises stress in the mandible bone (MPa)	Percentage of changes	The highest von Mises stress in the miniplate (MPa)	Percentage of changes	The maximum von Mises stress in the screws (MPa)	Percentage of changes (%)
Classic	162	-	526	-	330	-
Rectangle R1	149	8.02	306	41.8	216	34.56
Rectangle R2	119	26.54	345	34.4	222	32.72
Rectangle R3	121	25.3	400	23.95	253	23.63
Rectangle R4	114	29.6	294	44.1	196	40.6
Rectangle R5	119	26.54	357	32.12	196	40.6
Rectangle R6	119	26.54	327	37.83	206	37.57
Ellipse E1	144	11.11	457	13.11	301	20.17
Ellipse E2	144	11.11	442	15.96	247	25.15
Ellipse E3	129	20.37	383	27.18	235	28.78
Ellipse E4	135	16.66	410	22	228	30.9
Ellipse E5	157	3.08	205	23	240	27.27
Ellipse E6	158	2.46	467	11.21	248	24.84

Fig. 16 presents a bar chart comparing the relative displacement values between the two fractured surfaces in the mandible when using rectangular miniplates compared to classical (classic) miniplates. The relative displacement for the classical miniplate is 0.272 (mm). The relative displacement decreases in all six cases where the new design rectangular miniplates are employed for mandibular fracture fixation compared to when using the classic miniplate. Among the six rectangular miniplates, plate R3 produces the minimum relative displacement of 0.246 (mm), representing a 9.55% reduction compared to the classic miniplate displacement.

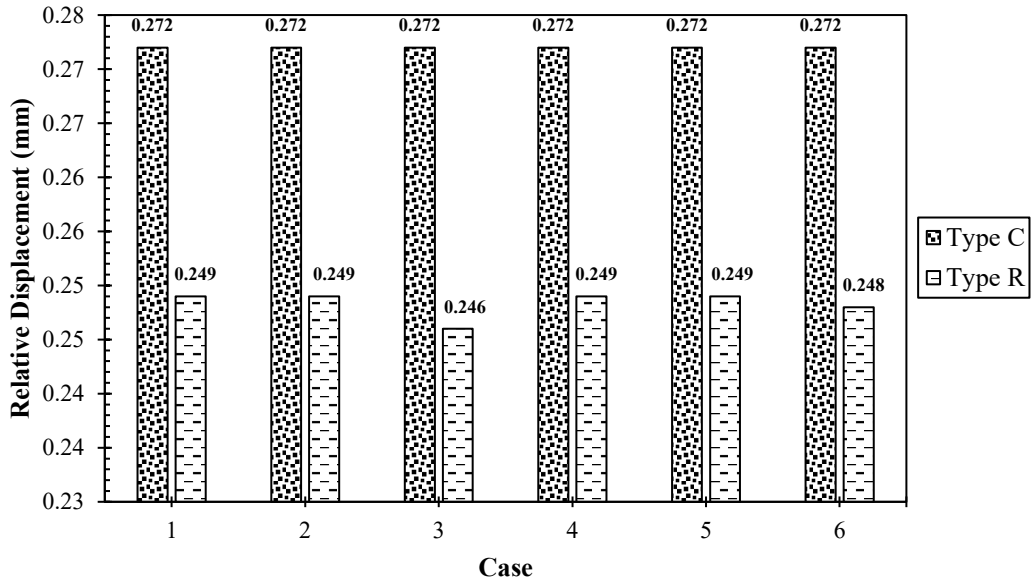


Fig. 16. Relative displacement values between the two fractured surfaces when using rectangular miniplates compared to classic miniplate.

Similarly, Fig. 17 shows a bar chart comparing the relative displacement values between the two fractured surfaces in the mandible when using elliptical miniplates with the relative displacement of the miniplate classic. As evident from Fig. 17, except for one case, the relative displacement between the fractured mandibular surfaces is smaller than when elliptical miniplates were used compared to the Classic miniplate. The minimum displacement is achieved with the E3 miniplate, with a value of 0.230 (mm), indicating a 15.4% reduction compared to the Classic miniplate relative displacement.

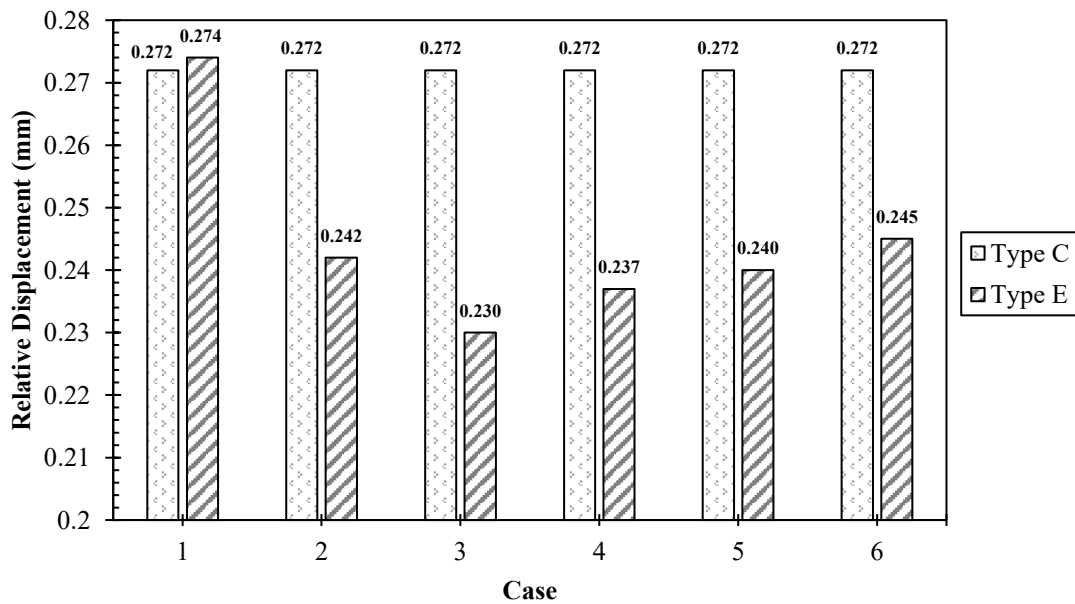


Fig. 17. Relative displacement values between the two fractured surfaces when using elliptical miniplates compared to classic miniplate.

Based on the observed trends in the relative displacement values for the new rectangular and elliptical miniplate designs, as presented in Fig. 16 and Fig. 17, it is evident that the elliptical miniplate design exhibits more significant sensitivity to geometric parameter variations compared to the rectangular miniplate design. This heightened sensitivity emphasizes the importance of precise geometric parameter selection and dimensional accuracy during the manufacturing process for elliptical miniplates.

Open surgery remains a cornerstone approach for restoring normal mandibular function after fractures. Precise and expeditious surgical techniques are critical for minimizing patient pain and accelerating recovery. This study investigates the mechanical behavior of fractured human mandibles using finite element analysis, focusing on novel elliptical miniplate designs for improved fixation. Thirteen different fixation scenarios were evaluated, including a conventional approach employing two classic miniplates secured with eight screws around the fracture site. Two novel rectangular and elliptical miniplate geometries were proposed, utilizing only six screws per plate. Muscle forces acting on the mandible were determined based on previous studies and applied to designated anatomical locations. The resulting stress levels within the mandible and miniplates were calculated. Four key performance indicators were used to assess the effectiveness of the miniplate designs with the following priorities:

- **Relative Displacement:** This criterion quantifies the movement between fractured bone segments, directly impacting stability and healing potential.
- **Von Mises Stress Reduction in Fracture Zone:** Minimizing stress in the fracture zone promotes healing and reduces re-fracture risk.
- **Stress in Miniplate:** Maintaining low-stress levels within the miniplate ensures its integrity and prevents material failure.
- **Stress in Screws:** Reduced screw stress minimizes loosening and fatigue failure.

The analysis revealed the superior performance of the proposed rectangular miniplate R3 and elliptical miniplate E3 designs compared to the conventional classic miniplate across all four performance indicators. The R3 design achieved the relative displacement (0.246 mm), signifying better stability than the classic miniplate. The E3 design achieved the lowest relative displacement (0.230 mm), signifying superior stability. Additionally, it demonstrated a significant reduction in von Mises stress within the highest von Mises stress in the mandible bone (20.37%), the highest von Mises stress in the mini plate (27.18%), and the maximum von Mises stress in the screws (28.78%), compared to the conventional miniplate classic.

The reduced number of screws in the new designs (6 compared to 8) aims to minimize iatrogenic bone damage during fixation. While this biomechanical improvement could theoretically contribute to a more favorable healing environment and potentially influence patient recovery, direct clinical evidence regarding faster recovery, or specific aesthetic and functional improvements, is beyond this computational study and further research, including clinical trials, is needed to confirm such clinical advantages.

Beyond the immediate benefit of reduced iatrogenic damage, the observed biomechanical advantages theoretically influence the incidence of certain postoperative complications. For instance, the lower von Mises stresses identified in the screws of the novel designs (Table 6 and Fig. 15) could potentially reduce the risk of screw loosening or fatigue failure over time, which are recognized hardware-related issues. Similarly, the enhanced stability at the fracture site, indicated by reduced relative displacement with the R3 and E3 designs (Figs 16 and 17), is fundamental for undisturbed bone healing. Improved stability may theoretically contribute to a lower risk of delayed union, non-union, or malunion. These healing disturbances can, in turn, predispose patients to further complications such as infection or the need for secondary surgical interventions. While this study did not directly quantify complication rates, these theoretical links, based on established biomechanical principles, warrant consideration and further investigation in clinical settings.

Although economic considerations and cost analysis are beyond the scope of this study, it is plausible that if the novel designs lead to a reduction in complication rates or a decreased necessity for revision surgeries they could potentially offer long-term cost benefits. Such an assessment would require dedicated health economic studies based on future clinical trial data.

It should be emphasized that the present study is a computational analysis, and its findings, while indicative of biomechanical advantages, will require further clinical and laboratory studies to substantiate these FEA results and to rigorously assess the long-term performance of the E3 miniplate design in a real-world clinical environment. This study demonstrates the computational promise of novel elliptical miniplate designs for mandibular fracture fixation, particularly the E3 design. Their superior simulated mechanical behavior suggests potential clinical advantages, which warrant thorough investigation and clinical evaluation to ascertain their real-world efficacy. Furthermore, the modeling of the bone-plate-screw interface assumed simplified contact conditions, and complex biological phenomena such as osseointegration, tissue healing, and potential micromotion at the interface over time were not simulated.

The fracture was modeled as a simple, linear gap, and patient-specific trauma segmentation or fracture propagation was not simulated. The loading conditions, while based on established literature, represent a specific biting task (symmetrical bilateral clenching) and do not encompass the full dynamic range of masticatory forces or parafunctional activities that a patient might experience. Furthermore, this study did not directly assess or quantify the incidence of specific clinical complications (such as screw loosening or plate exposure), nor did it conduct a cost analysis of the proposed designs compared to conventional methods. Such evaluations are crucial for a complete understanding of their clinical utility and fall within the scope of future research, including the assessment of long-term aesthetic outcomes and the incidence of revision surgery. Additionally, the mandible model was constructed from CBCT data of a single 30-year-old male patient and thus does not account for anatomical variability related to sex, age, bone density, or specific fracture characteristics (such as comminution or bone loss). This research provides valuable insights into the potential biomechanical benefits of novel elliptical miniplate designs, paving the way for future translational research in this field.

4. Conclusions

This study utilized Finite Element Analysis to evaluate the biomechanical performance of novel rectangular and elliptical miniplate designs for mandibular symphyseal fracture fixation, comparing them with a conventional two-plate technique. The key findings indicate that:

- Both novel rectangular (specifically design R3) and elliptical (specifically design E3) miniplates demonstrated a reduction in relative displacement at the fracture site compared to the classic miniplate configuration, suggesting enhanced stability. The E3 elliptical design showed the most significant reduction (15.4%).
- The novel designs achieved this improved stability with fewer screws (six versus eight), which implies less iatrogenic bone damage.
- Von Mises stresses in the mandible bone, the miniplates themselves, and the fixation screws were generally lower or comparable with the novel designs, particularly for the optimized R3 and E3 configurations, indicating a favorable stress distribution.

These computational results suggest that the proposed novel miniplate geometries, particularly the R3 rectangular and E3 elliptical designs, offer promising biomechanical advantages over

conventional fixation methods for mandibular symphyseal fractures. They provide a strong biomechanical rationale for potentially improved clinical outcomes. However, as this is a computational investigation, further comprehensive experimental validation (including mechanical testing of prototypes and clinical trials) is crucial to confirm these potential benefits, assess their long-term performance, and evaluate their overall suitability for clinical application. The insights gained from this study pave the way for future translational research aimed at developing more effective and less invasive fixation systems for mandibular fractures.

Conflicts of Interest Statement

The authors declare that there are no financial or non-financial conflicts of interest related to this work.

Funding

This research did not receive any specific grant from funding agencies in the public, commercial, or non-profit sectors.

Generative AI Declaration

The authors declare that no generative AI and AI-assisted technologies have been used in the writing process of this paper.

References

1. Knoll W-D, Gaida A, Maurer P. Analysis of mechanical stress in reconstruction plates for bridging mandibular angle defects. *Journal of Cranio-Maxillofacial Surgery*. 2006;34(4):201-209.
2. Kolsuz N, Atali O, Varol A. Assessment of biomechanical properties of specially-designed miniplate patterns in a mandibular subcondylar fracture model with finite element analysis and a servohydraulic testing unit. *British Journal of Oral and Maxillofacial Surgery*. 2020;58(7):848-853.
3. Farwell DG. Management of symphyseal and parasymphyseal mandibular fractures. *Operative Techniques in Otolaryngology-Head and Neck Surgery*. 2008;19(2):108-112.
4. Ellis Iii E, Moos KF, El-Attar A. Ten years of mandibular fractures: an analysis of 2,137 cases. *Oral surgery, oral medicine, oral pathology*. 1985;59(2):120-129.
5. Gear AJL, Apasova E, Schmitz JP, Schubert W. Treatment modalities for mandibular angle fractures. *Journal of oral and maxillofacial surgery*. 2005;63(5):655-663.
6. Alkan A, Çelebi N, Özden B, Baş B, İnal S. Biomechanical comparison of different plating techniques in repair of mandibular angle fractures. *Oral Surgery, Oral Medicine, Oral Pathology, Oral Radiology, and Endodontology*. 2007;104(6):752-756.
7. Chiodo TA, Ziccardi VB, Janal M, Sabitini C. Failure strength of 2.0 locking versus 2.0 conventional Synthes mandibular plates: a laboratory model. *Journal of oral and maxillofacial surgery*. 2006;64(10):1475-1479.
8. Moore GF, Olson TS, Yonkers AJ. Complications of mandibular fractures: A retrospective review of 100 fractures in 56 patients. *The Nebraska medical journal*. 1985;70(4):120-123.

9. Fedok FG, Van Kooten DW, DeJoseph LM, et al. Plating techniques and plate orientation in repair of mandibular angle fractures: an in vitro study. *The Laryngoscope*. 1998;108(8):1218-1224.
10. Park I-P, Heo S-J, Koak J-Y, Kim S-K. Post traumatic malocclusion and its prosthetic treatment. *The Journal of Advanced Prosthodontics*. 2010;2(3):88-91.
11. Fox AJ, Kellman RM. Mandibular angle fractures: two-miniplate fixation and complications. *Archives of facial plastic surgery*. 2003;5(6):464-469.
12. Aggarwal S, Singh M, Modi P, Walia E, Aggarwal R. Comparison of 3D plate and locking plate in treatment of mandibular fracture—a clinical study. *Oral and maxillofacial surgery*. 2017;21:383-390.
13. Li J, Jiao J, Luo T, Wu W. Biomechanical evaluation of various internal fixation patterns for unilateral mandibular condylar base fractures: A three-dimensional finite element analysis. *Journal of the Mechanical Behavior of Biomedical Materials*. 2022;133:105354.
14. Korkmaz HH. Evaluation of different miniplates in fixation of fractured human mandible with the finite element method. *Oral Surgery, Oral Medicine, Oral Pathology, Oral Radiology, and Endodontology*. 2007;103(6):e1-e13.
15. Arbag H, Korkmaz HH, Ozturk K, Uyar Y. Comparative evaluation of different miniplates for internal fixation of mandible fractures using finite element analysis. *Journal of oral and maxillofacial surgery*. 2008;66(6):1225-1232.
16. Van Eijden T, Korfage JAM, Brugman P. Architecture of the human jaw-closing and jaw-opening muscles. *The Anatomical Record: An Official Publication of the American Association of Anatomists*. 1997;248(3):464-474.
17. Koolstra JH, Van Eijden T, Van Spronsen PH, Weijs WA, Valk J. Computer-assisted estimation of lines of action of human masticatory muscles reconstructed in vivo by means of magnetic resonance imaging of parallel sections. *Archives of Oral Biology*. 1990;35(7):549-556.
18. Cattaneo PM, Kofod T, Dalstra M, Melsen B. Using the finite element method to model the biomechanics of the asymmetric mandible before, during and after skeletal correction by distraction osteogenesis. *Computer Methods in Biomechanics and Biomedical Engineering*. 2005;8(3):157-165.
19. Kummer FJ. Craniomaxillofacial bone healing, biomechanics, and rigid internal fixation. *Craniomaxillofacial Reconstructive and Corrective Bone Surgery: Principles of Internal Fixation Using the AO/ASIF Technique*: Springer; 2002.
20. Koriath TWP, Versluis A. Modeling the mechanical behavior of the jaws and their related structures by finite element (FE) analysis. *Critical Reviews in Oral Biology & Medicine*. 1997;8(1):90-104.
21. Nelson GJ. Three dimensional computer modeling of human mandibular biomechanics. 1986.
22. Koriath TWP, Hannam AG. Deformation of the human mandible during simulated tooth clenching. *Journal of dental research*. 1994;73(1):56-66.
23. Caraveo V, Lovald S, Khraishi T, Wagner J, Baack B. The effects of frictionless/frictional contact boundary conditions in finite element modeling of mandibular fractures. *Multidiscipline Modeling in Materials and Structures*. 2008;4(3):227-236.
24. Lovald ST, Khraishi T, Wagner J, Baack B, Kelly J, Wood J. Comparison of plate-screw systems used in mandibular fracture reduction: finite element analysis. 2006.
25. Lovald ST, Wagner JD, Baack B. Biomechanical optimization of bone plates used in rigid fixation of mandibular fractures. *Journal of oral and maxillofacial surgery*. 2009;67(5):973-985.
26. Koriath TWP, Romilly DP, Hannam AG. Three-dimensional finite element stress analysis of the dentate human mandible. *American journal of physical anthropology*. 1992;88(1):69-96.
27. Tate GS, Ellis Iii E, Throckmorton G. Bite forces in patients treated for mandibular angle fractures: implications for fixation recommendations. *Journal of oral and maxillofacial surgery*. 1994;52(7):734-736.
28. Gray LE, Ostby JS. In utero 2, 3, 7, 8-tetrachlorodibenzo-p-dioxin (TCDD) alters reproductive morphology and function in female rat offspring. *Toxicology and applied pharmacology*. 1995;133(2):285-294.

29. Caraveo V, Lovald S, Khraishi T. A study of the mechanical characteristics of a mandibular parasymphiseal fracture with internal fixation device subject to variable bite forces: finite element analysis. *Journal of Biosciences and Medicines*. 2021;9(04):158.
30. Shemtov-Yona K, Rittel D. An overview of the mechanical integrity of dental implants. *BioMed research international*. 2015;2015(1):547384.
31. Hong DGK, Oh J-h. Recent advances in dental implants. *Maxillofacial Plastic and Reconstructive Surgery*. 2017;39(1):33.
32. Darvish D, Khorrammehr S, Nikkhoo M. Finite Element Analysis of the Effect of Dental Implants on Jaw Bone under Mechanical and Thermal Loading Conditions. *Mathematical Problems in Engineering*. 2021;2021(1):9281961.
33. Elias CN, Fernandes DJ, Souza FMd, Monteiro EdS, Biasi RSd. Mechanical and clinical properties of titanium and titanium-based alloys (Ti G2, Ti G4 cold worked nanostructured and Ti G5) for biomedical applications. *Journal of Materials Research and Technology*. 2019;8(1):1060-1069.
34. Pinheiro M, Alves JL. The feasibility of a custom-made endoprosthesis in mandibular reconstruction: Implant design and finite element analysis. *Journal of Cranio-Maxillofacial Surgery*. 2015;43(10):2116-2128.
35. W. Nicholson J. Titanium Alloys for Dental Implants: A Review. *Prosthesis*. 2020;2(2):100-116.
36. Hu H, Xu Z, Dou W, Huang F. Effects of strain rate and stress state on mechanical properties of Ti-6Al-4V alloy. *International Journal of Impact Engineering*. 2020;145:103689.
37. Bozkaya D, Muftu S, Muftu A. Evaluation of load transfer characteristics of five different implants in compact bone at different load levels by finite elements analysis. *The Journal of prosthetic dentistry*. 2004;92(6):523-530.